Eur. Phys. J. Plus (2015) **130**: 43
DOI 10.1140/epjp/i2015-15043-3

THE EUROPEAN PHYSICAL JOURNAL PLUS

Regular Article

Status of the crystallography beamlines at Elettra*

A. Lausi[1,a], M. Polentarutti[1], S. Onesti[1], J.R. Plaisier[1], E. Busetto[1], G. Bais[1], L. Barba[2], A. Cassetta[2], G. Campi[3], D. Lamba[2], A. Pifferi[3], S.C. Mande[4], D.D. Sarma[5], S.M. Sharma[6], and G. Paolucci[1]

[1] Elettra - Sincrotrone Trieste S.C.p.A., S.S. 14 km 163,5 in AREA Science Park - loc. Basovizza, 34149 Trieste, Italia
[2] Istituto di Cristallografia - UOS di Trieste, Consiglio Nazionale delle Ricerche, S.S. 14 km 163,5 in AREA Science Park - loc. Basovizza, 34149 Trieste, Italia
[3] Istituto di Cristallografia - UOS di Monterotondo, Consiglio Nazionale delle Ricerche, Area della Ricerca di Roma, Via Salaria Km 29.300, I-00015 Monterotondo (Roma), Italia
[4] National Centre for Cell Science, Ganeshkhind, Pune-411 007, India
[5] Solid State and Structural Chemistry Unit, Indian Institute of Science, Bangalore 560012, India
[6] High Pressure & Synchrotron Radiation Physics Division, Bhabha Atomic Research Centre, Mumbai 400 085, India

Received: 3 February 2015
Published online: 12 March 2015 –

Abstract. Elettra is one of the first 3rd-generation storage rings, recently upgraded to routinely operate in top-up mode at both 2.0 and 2.4 GeV. The facility hosts four dedicated beamlines for crystallography, two open to the users and two under construction, and expected to be ready for public use in 2015. In service since 1994, XRD1 is a general-purpose diffraction beamline. The light source for this wide (4–21 keV) energy range beamline is a permanent magnet wiggler. XRD1 covers experiments ranging from grazing incidence X-ray diffraction to macromolecular crystallography, from industrial applications of powder diffraction to X-ray phasing with long wavelengths. The bending magnet powder diffraction beamline MCX has been open to users since 2009, with a focus on microstructural investigations and studies under non-ambient conditions. A superconducting wiggler delivers a high photon flux to a new fully automated beamline dedicated to macromolecular crystallography and to a branch beamline hosting a high-pressure powder X-ray diffraction station (both currently under construction). Users of the latter experimental station will have access to a specialized sample preparation laboratory, shared with the SISSI infrared beamline. A high throughput crystallization platform equipped with an imaging system for the remote viewing, evaluation and scoring of the macromolecular crystallization experiments has also been established and is open to the user community.

1 Introduction

Elettra Sincrotrone Trieste is an international research centre hosting two different synchrotron light sources: Elettra, a third-generation storage ring after which the centre itself is named [1], and FERMI, a cutting-edge free electron laser (FEL) [2,3]. The light produced is collected and conveyed to over 30 experimental stations, which use it as their main tool for analysis, supported by laboratories specializing in chemistry, microscopy, materials science, electronics, and information technology.

Elettra has been in operation since October 1993. Working at 2.0 and 2.4 GeV, it has been optimised to provide the scientific community with photons in the energy range from a few to several tens of KeV with spectral brightness of up to 10^{19} photons/s/mm^2/mrad^2/0.1% bw (see fig. 1) and is continuously upgraded in order to be competitive with the most recent sources. In 2007 construction of a full energy injector was completed consisting of a small LINAC (LINear ACcelerator) and a full energy booster that accelerates and injects electrons at the final energy of 2 and 2.4 GeV. The 1 GeV old injector has been partially refurbished and is now part of the new 1.2–1.8 GeV FEL facility FERMI. Today Elettra operates in top-up mode at both 2 and 2.4 GeV energy and hosts 26 different operational beamlines, specialized in various types of analytical measurements ranging from diffraction to spectroscopy and from microscopy to tomographic imaging.

* Contribution to the Focus Point on "Status of third-generation synchrotron crystallography beamlines: An overview" edited by Gaston Garcia.

[a] e-mail: andrea.lausi@elettra.eu

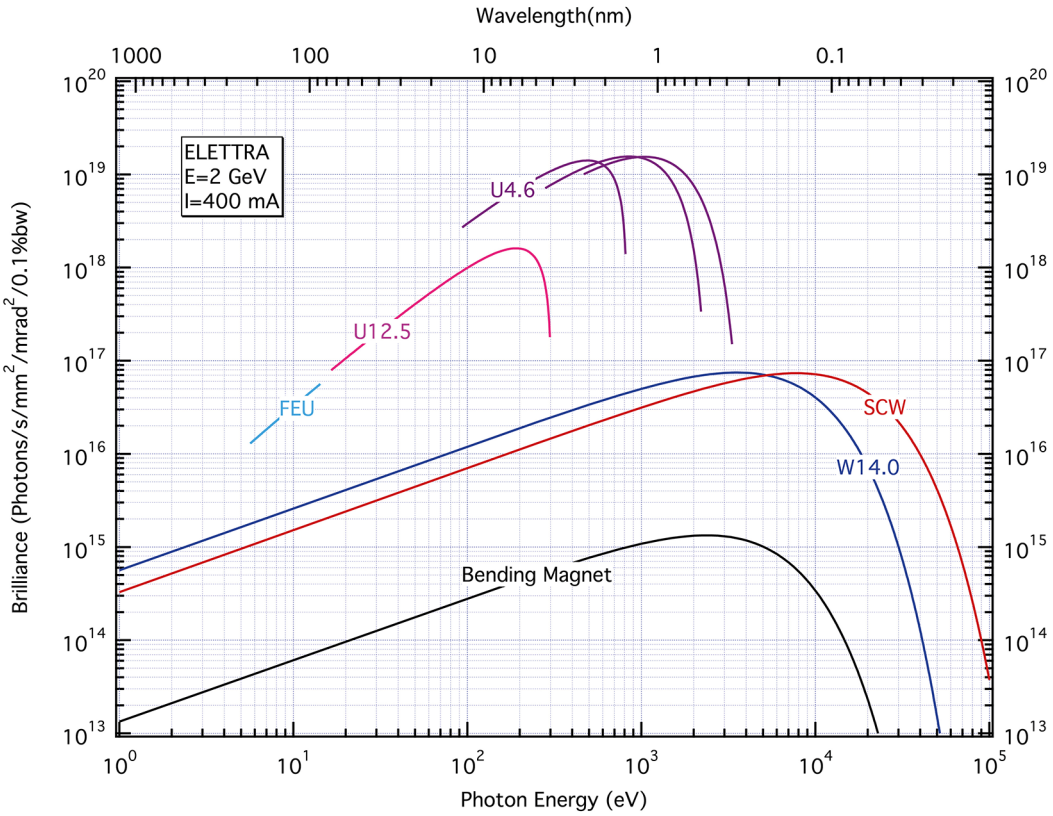

Fig. 1. Brilliance of the synchrotron radiation for various insertion devices and for bending magnets at Elettra as a function of photon energy.

Access to the facilities is offered based on scientific merit. According to the access procedure, users submit the experiment proposals through the VUO (Virtual Unified Office) `https://vuo.elettra.eu/`.

There are two proposal submission deadlines per year, mid-March and mid-September. The proposals are evaluated by an international peer review panel, and those selected are allocated on the assigned beamline. Macromolecular crystallography proposals can be submitted anytime; there is no deadline for the submission and the evaluation is monthly.

The centre plays a leading role in the development of joint projects between European research facilities: Elettra is the coordinator of the networks promoting transnational access to synchrotrons and free electron lasers, the development of shared activities, and the strengthening of services provided to clients. Elettra is also an associate of IAEA, the International Atomic Energy Agency, and is part of the primary science and technology network of the Central European Initiative (CEI).

2 Beamlines dedicated to crystallography

2.1 Overview

Elettra hosts 4 beamlines dedicated to crystallography. XRD1 [4] was part of the phase one set of beamlines at Elettra and is open to users since 1996 as a general-purpose diffraction beamline. Over the years it has hosted both macromolecular crystallography and materials science experiments.

Using a bending magnet as the source, the powder diffraction beamline MCX [5] is dedicated mainly to microstructural characterization of materials. MCX has been open to users since 2009.

In order to extend the experimental capabilities of the facility towards high energy, a superconducting wiggler has recently been installed as a source for a cluster of diffraction beamlines. These will serve the wide communities of structural biology and physics at extreme conditions. The first two beamlines of the cluster, XRD2 [6] and Xpress [7], have been designed and constructed in collaboration with the Indian Institute of Science in Bangalore and will be open to users in 2015. The cluster will be further extended with a beamline, Pharma, dedicated to proprietary pharmaceutical research.

Table 1. Summary of the diffraction beamlines at Elettra.

Beamline	Application	User operation from	Source	Energy (keV)	Flux (ph/s @12 keV) at sample position	Spot size H × V (μm)
XRD1	General-purpose crystallography and scattering	1996	W14	4–21.5	10^{12}	700 × 300
MCX	Powder diffraction	2009	BM	6–22	10^{10}	300 × 300
XRD2	Macromolecular crystallography	2015	SCW	8–35	10^{13}	280 × 90
Xpress	High-pressure diffraction	2015	SCW	25	10^{11}	80 × 80

An overview of the four beamlines is given in table 1.

To support and complement the macromolecular crystallography activities in the last few years Elettra has invested in the development of a well-equipped structural biology laboratory, including state-of-the-art facilities for cloning, protein expression in bacterial, insect and mammalian cells, protein purification, biochemical and biophysical characterization and crystallization of macromolecules and macromolecular complexes. The laboratory also includes an automated high-throughput crystallization suite comprising liquid handlers and a crystallization robot. Two storage and imaging systems for the automatic visualization and recording of crystallization experiments are available with a capability of 430 Medical Research Council (MRC) plates.

The crystallization facility is open to external users worldwide via the Elettra's VUO webpage offering web-based remote monitoring of crystallization experiments.

To support the Xpress beamline activities a laboratory equipped with different kind of diamond anvil cells, helium load system setup, pressure gauge and gasket and sample preparation tools has been implemented.

2.2 XRD1 – an X-ray diffraction general-purpose beamline

The beamline [8] exploits a multipole wiggler (W14, see fig. 1) as radiation source. The beamline optics underwent a substantial upgrade in 2007 and consist now of a vertical collimating mirror and of a bendable focusing mirror upstream and downstream the monochromator. The size of the focal spot and the angular divergences are 700 μm × 300 μm (FWHM) and 2.3 mrad × 0.3 mrad (FWHM), respectively. The Si(111) double-crystal monochromator has a bandpass of a few eV in the broad spectrum of 4.0–21.5 keV. Time-resolved, white beam experiments are also possible.

The flexible setup consisting of a 3-circle "kappa" geometry goniostat equipped with a choice X-ray detectors and a robotic arm to handle various kind of samples, permits to host different experiments, ranging from single-crystal to powder diffraction, in scientific fields as diverse as macromolecular crystallography and materials science at ambient or extreme conditions.

In particular, the equipment comprises a fast-readout, large-area hybrid detector (2M Pilatus from DECTRIS) and a CCD area detector (MarCCD165) located on a 2-theta arm. A 25 mm^2 silicon pin diode detector (X123 from Amptek) is used to detect fluorescence signal from samples.

A custom developed sample mounting robot with a capacity of 50 samples is available for both single-crystal and powder diffraction experiments. The system is capable to automatically select, mount and align in the X-ray beam samples at both room and cryogenic (liquid nitrogen) temperatures, typical of macromolecular crystallography. The sample changer is based on the SPINE standardized support and ESRF pucks [9]. Sample tracking is ensured by a 2D barcode reading system.

Dedicated software to collect diffraction data from single-crystal and powder diffraction exists together with a flexible, object-oriented scripting protocol to easily implement more complex experiments without requiring a detailed knowledge of the beamline software and hardware. Remote data collection is possible in presence of a minimal network bandwidth of 3 Mb/s at the client site.

2.3 MCX – Powder diffraction beamline

The materials characterization by X-ray diffraction (MCX) beamline is dedicated to diffraction studies from polycrystalline materials, surfaces, thin films, and coatings. The three-element optical configuration (collimating mirror/double-crystal monochromator with sagittal focusing/bendable focussing mirror) allows to deliver photon flux values of interest for specific experiments in the range between 6 and 22 keV.

MCX makes a wide spectrum of measurements available at an Elettra Bending Magnet, comprising powder diffraction (also in non-ambient conditions), thin film and grazing angle diffraction, surface and thin films reflectivity, texture, stress, strain measurements and reciprocal space mapping. The flexibility of the beamline optics set-up allows selecting between a high angular resolution (parallel beam) and a high flux (converging beam - point focus) configuration.

The station is based on a 4-circle diffractometer (Huber - 2theta precision better than 0.0001°) in full circle configuration with a flat sample-holder plate (Ø 100 mm) controlled by a precision (1 μm) x-y-z motor system, 360° phi-rotation and −90–+90° chi-tilting. The 2theta rotation is provided with an optical encoding system for accurate control and real-time feedback on the actual angular positions.

In standard operating conditions, in order to maximize the flux at the detector, MCX operates by focusing the beam both in the vertical and in the horizontal plane at the detector and the instrumental peak profile is around 0.018° at 15 keV. The vertical divergence is controlled by acting on the second (bendable) mirror, whereas the horizontal divergence is managed by acting on the second (also bendable) crystal of the monochromator. The beam spot at the experiment can be varied from point focus ($0.3 \times 0.3\,\mathrm{mm}^2$), to line focus ($5 \times 1\,\mathrm{mm}^2$). The diffracted beam is collimated by setting the slits at an aperture of 0.1 mm, to limit the effects of axial divergence. At the expense of photon density, defocusing the second mirror allows narrowing the instrumental peak profile down to 0.012° [10].

A second experimental set-up based on a furnace [11] is also available to provide an atmosphere and temperature controlled environment, up to 1000 °C, for powders in capillaries and a temperature controlled environment for thin-film samples. The powder pattern is recorded by a translating image plate, as a fast data collection system to follow phase transformations and chemical reactions.

2.4 The SCW beamline cluster

As a result of a joint project between the Indian Institute of Science (Bangalore) and Elettra Sincrotrone Trieste a group of new crystallographic beamlines will be opened to the users in 2015. The project exploits the wide angular span of X-rays produced by a 3.5 T superconducting wiggler (SCW). The emission fan from the wiggler is sectioned and used to deliver in parallel the beam to three beamlines: the central one, XRD2 (see sect. 3), is tunable in the range 8–35 keV, while the right and left branches select energies of 25 keV, Xpress, and 13 keV, Pharma (see sect. 2.5), respectively.

2.4.1 The Xpress branch line

The fixed-energy branch line Xpress is dedicated to angle-dispersive diffraction experiments at extreme conditions. The beamline uses one single, 30 mm thick, slab of silicon cut along the (111) face to intercept the beam from the source and focuses it to the experimental station by means of a platinum coated toroidal mirror.

The expected spot size at the sample is 500 μm × 200 μm (FWHM) at 2.4 GeV and 140 mA with a photon flux of 10^{11} ph/s in a 80 μm × 80 μm aperture. The angular divergence is 0.65 mrad × 0.25 mrad (FWHM) and the energy bandpass about 10^{-3}.

The experimental setup consists of a large area detector (Mar345 imaging plate) and an on-line spectrometer for pressure calibration based on ruby fluorescence. It can host different kind of high-pressure diamond cells (Mao-Bell, Merrill-Bassett, membrane-driven Boehler). A helium gas loader is expected to be available since the beginning of the beamline activity in 2015, while a laser heating upgrade is foreseen for 2016.

2.5 Future developments and upgrades

Pharma, the second branch line from the superconducting wiggler, is expected to be implemented in the near future to support specific industrial and pharmaceutical activities already present at Elettra and related, in particular, to the crystalline forms of active pharmaceutical ingredients.

Also planned for the near future (2015) is the implementation of a new liquid nitrogen cooling system for the monochromator of the XRD1 beamline. This will allow to substantially reduce the focus size, and increase up to one order of magnitude the beamline flux at the sample. A spectroscopic characterization of the samples is also being implemented at XRD1 to be used in parallel with the diffraction data collection.

3 The XRD2 Macromolecular crystallography beamline

The exponential growth of structural biology has driven the need for crystallographic beamlines which provide rapid and efficient access to brilliant tunable X-ray sources. The availability of such sources has in turn generated a significant impact on biology, impact measured in terms of both number and complexity of the macromolecular structures determined.

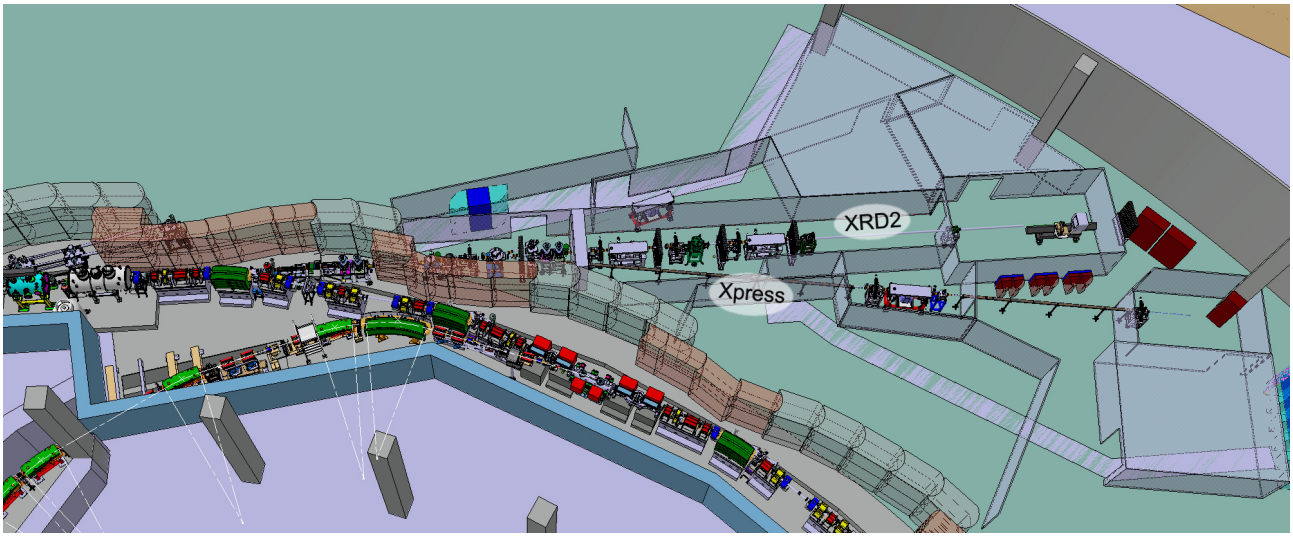

Fig. 2. 3D rendering of the SCW cluster of beamlines with the optical elements of XRD2 and Xpress.

Table 2. Estimated fluxes at the sample (ph/s @12 keV) at XRD2, considering the reflectivity and bandwith of the monochromator and the reflectivity of the two mirrors.

Size	Flux @2 GeV, 310 mA	Flux @2.4 GeV, 140 mA
$200\,\mu\text{m} \times 200\,\mu\text{m}$	2×10^{13}	3.1×10^{13}
$50\,\mu\text{m} \times 50\,\mu\text{m}$	1.7×10^{12}	2.5×10^{12}
$10\,\mu\text{m} \times 10\,\mu\text{m}$	0.5×10^{11}	0.8×10^{11}

The XRD2 beamline (see fig. 2) will offer a high photon flux at high energies, and will be complementary to XRD1, whose X-ray spectrum reaches a maximum intensity in the range below 8 keV. As a matter of fact, the combination of the two beamlines offers the possibility to access all the atomic edges used in SAD/MAD experiments to overcome the phase problem (starting from the calcium K-edge) and allows the exploitation of anomalous signal enhancement from biologically relevant elements like manganese, potassium, chlorine, iodine, calcium, sulfur and many others.

The main optical components of XRD2 consist of a platinum-coated vertical collimating mirror, a double-crystal monochromator in non-dispersive configuration and a focusing mirror (see fig. 2). The size of the focal spot and the relative angular divergences are $90\,\mu\text{m} \times 300\,\mu\text{m}$ (FWHM) and $2.0\,\text{mrad} \times 0.25\,\text{mrad}$ (FWHM), respectively. Estimated fluxes through a slits-limited aperture at the focal plane are reported in table 2, where the reflectivity of the mirrors and the efficiency of the monochromator have been considered.

The experimental setup consists of a large-area hybrid detector (6M Pilatus from DECTRIS) and a MD2 microdiffractometer from Bruker, equipped with a minikappa goniometer. A silicon pin diode (Amptek X123) is used to collect the needed data for SAD/MAD experiments. The sample changer, similar to the one available on the XRD1 beamline, will be able to host both SPINE and MINISPINE sample holders. Remote data collection will be available to the users.

4 Examples of science at crystallography beamlines

4.1 Evolution and control of oxygen order in a cuprate superconductor

Materials science researchers have always exploited the XRD1 beamline, mainly for the combination of a high-brilliance X-ray beam with tunable beam energy and a bidimensional detector which allow for flexible and less time-consuming experiments. Proposed experiments, among others, dealt with the characterization of pressure, temperature or photon-induced crystallographic phase transitions on a variety of materials classes. After the beamline upgrade this kind of experiments are even less limited by factors like sample dimensions and dynamic range of the detector. Moreover, the improved automatized sample orientation together with the availability of more degrees of freedom, have attracted a new research community aiming at characterizing soft matter, and in particular thin films of organic semiconductors by grazing incidence X-ray diffraction techniques.

A challenging field well represented in XRD1 scientific output of the last years is the characterization of multiscale phase separation in transition metal oxides, such as high-temperature superconductors. Phase separation in these compounds is due to the specific arrangement of defects in nanodomains, causing the presence of weak and/or diffuse

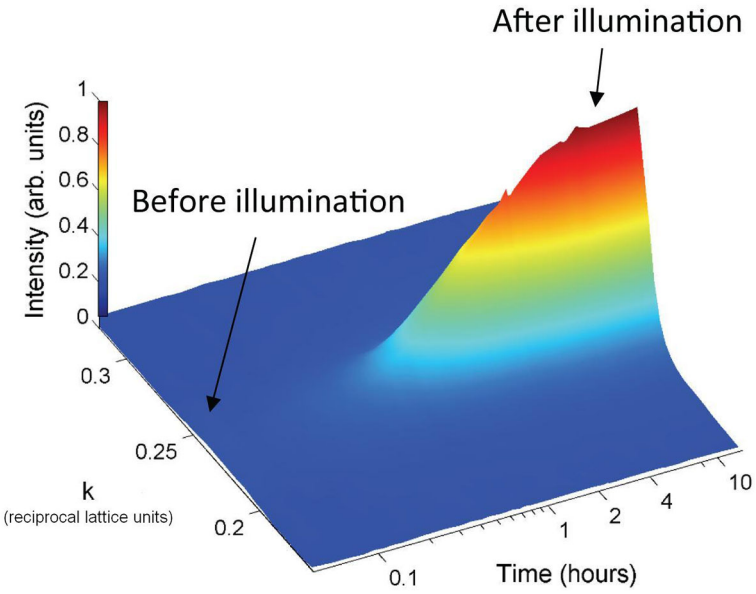

Fig. 3. Defects ordering monitored by the growth of satellite peak profile $q_{\mathrm{oxy}} = (0.89, \mathrm{k}, 6)$ during X-ray exposure at constant X-ray photon flux $\Phi = 5 \times 10^{14}\,\mathrm{s}^{-1}\,\mathrm{cm}^{-2}$ photons with wavelength of 1 Angstrom, at fixed temperature of 250 K. Before illumination, the disordered phase has been obtained by quenching the sample from $T = 350\,\mathrm{K}$, where the oxygen defects get disordered, down to 250 K.

scattering such as satellite peaks, streaks, etc., around the spots of the primary diffraction pattern. Since the defects organization controls the electronic functionalities, the ability to manipulate and control their arrangement is of paramount importance. As an example, Poccia *et al.* [12] described the possibility to control the disposition of defects, mobile interstitial oxygen atoms, y, in the La_2CuO_{4+y} superconducting cuprate, through X-ray illumination (fig. 3). More specifically, a controlled X-ray flux has been used for photo-switching the disorder to order transition of defects. The authors associated the higher ordering degree of defects with the onset of higher-quality superconductivity in the illuminated zones of the sample. This led to the development of novel technological tools based on the use of X-ray beams as a pen, to design arbitrary patterns of higher superconducting paths for advanced materials functionality.

4.2 Multi-target-directed ligands in Alzheimer's disease treatment: A structure-based drug discovery story

Alzheimer's disease (AD), which is the most common cause of senile dementia, is a major public health issue with devastating economic and human impacts. AD is clinically characterized by a loss of memory and cognition that is associated with deterioration of the basal forebrain cholinergic neuronal network, resulting in a reduction in the level of the neurotransmitter acetylcholine. Although several treatment strategies have been proposed most current therapeutic options involve restoring acetylcholine levels in the brain. AChE (acetylcholinesterase) inhibitors donepezil, rivastigmine and galanthamine are currently approved anti-AD drugs. The complex aetiology of AD has prompted us to the development of multi-target-directed ligands (MTDLs) that act simultaneously on different components of AD pathology, *e.g.* the cholinergic dysfunction, amyloid plaques, neurofibrillary tangles, inflammatory intermediates and reactive oxygen species. One strategy currently being explored for the development of new therapeutics for AD involves linking tacrine, a known AChE inhibitor, to another drug or active molecule aimed at a different target. To aid in the design of these MTDLs, we have determined the crystal structure of TcAChE (*Torpedo californica* acetylcholinesterase) in complex with a 6-chlorotacrine-juglone hybrid ("I" in fig. 4). This compound shows inhibition of Aβ self-aggregation and AChE IC_{50} activities of $37.5 \pm 4.9\,\mu$M and $0.72 \pm 0.06\,$nM, respectively. Consequently, this compound emerged as a promising molecule for the therapy of Alzheimer's disease [13].

4.3 Tuning the growth mode of nanowires via the interaction among seeds, substrate and beam fluxes

The *in situ* reaction furnace at MCX has recently been equipped with a precise goniometer and a sample holder for thin film samples. This setup has been used to obtain important information about the physical state of Au nanoparticles (NPs) supported on GaAs wafers, of interest for the growth of ZnSe nanowires (NWs) [14].

Semiconductor nanowires are attracting increasing attention due to their novel properties that make them promising building blocks for electronic and optoelectronic devices. Their highly anisotropic growth originates from the presence of a metal nanoparticle seed, that acts as catalyst for the one dimensional crystal growth. The most common way adopted to generate the nanoparticles (NPs) is by dewetting a thin metal film deposited on the substrate. Size and

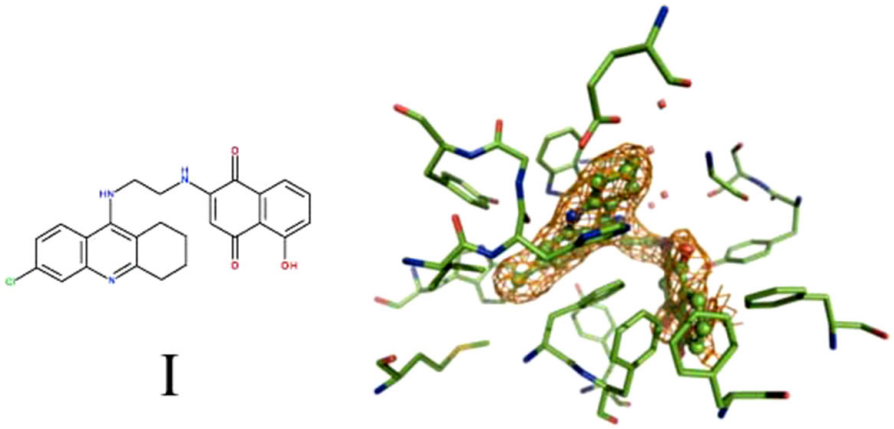

Fig. 4. Close-up view of the active site of *Tc*AChE in complex with (I). The final 2Fo - Fc σA-weighted electron density map, carved around (I), is contoured at 1.0σ.

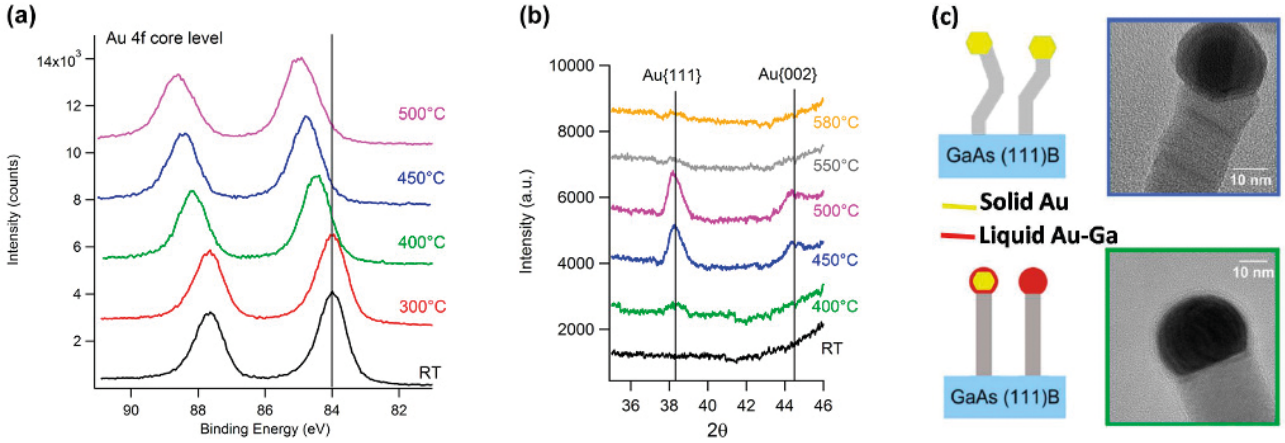

Fig. 5. (a) XPS 4f core level and (b) X-Ray diffraction peaks of the Au NPs as a function of the annealing temperature. (c) Schematic view of the different ZnSe NWs growth mechanisms and TEM images of the NW morphologies obtained under Zn-rich (top) and Se-rich (bottom) growth conditions at 450 °C.

physical state (liquid or solid) of the resulting NPs affect the subsequent NW growth mechanism, playing a crucial role in determining the properties of the NWs. Concerning ZnSe, the Au-assisted NW growth mechanism is still controversial. In order to reach a deeper understanding of the Au-assisted ZnSe NW growth on GaAs substrates, and get information about the physical state of the NPs, the NPs formation process has been studied by complementing information from *in situ* X-ray photoemission spectroscopy (XPS) performed in an analysis chamber connected with the molecular beam epitaxy system, with *ex situ* grazing incident X-ray diffraction as a function of temperature carried out at the MCX beamline. A progressive shift toward higher binding energy of the Au 4f core level XPS signal as the annealing temperature is increased above 400 °C reveals the occurrence of a thermal diffusion of Ga atoms from the substrate into the Au NPs, with the formation of a Au-Ga alloy phase. The Au 4f peak position and the Au-Ga phase diagram suggests that the Au-Ga alloy is liquid. However, the study of the process at MCX beamline revealed that Au diffraction peaks, absent at low temperatures because of the epitaxial nature of the metal, appear at 400 °C when the dewetting process begins to be effective and remain detectable up to 550 °C, indicating that only above this temperature the NPs melt completely. The results of XPS and X-ray diffraction analysis are reconciled supposing that the NPs obtained at 450 °C have a liquid Au-Ga alloy shell, and a solid core made of pure Au or Au-rich solid solution. Chemical composition and physical state of such NPs are strongly affected by the Se flux: when the NPs are exposed to Se, the Au 4f signal is back shifted toward the pure Au position, indicating that the Se beam reacts with the Ga atoms of the Au-Ga alloy NPs, draining them out of the particles and restoring the composition of pure Au nanocrystals, while the Zn beam does not alter the chemical composition of the Au-Ga NPs. These results elucidate what happens when ZnSe NWs grow at 450 °C in different flux conditions: using Zn-rich conditions, the NWs grow through the vapour-liquid-solid (VLS) mode, assisted by Au-Ga NPs either completely liquid or solid with a liquid shell. The NW are straight and uniformly oriented. If Se-rich conditions are used, Ga is drained out of the NPs and the NW growth mechanism is switched toward the vapour-solid-solid (VSS) mode, assisted by solid Au nanocrystals (see fig. 5). The NWs are kinked with a high density of defects.

5 Conclusions

X-ray crystallography and X-ray scattering techniques in general are present since the first stages of operation of the Elettra ring. With the start of operation of the superconducting wiggler cluster of beamlines, 2015 will represent a new milestone in the history of the facility. The new source will boost crystallography both in terms of number of dedicated beamlines and of availability of high fluxes at high photon energies. The activities of the new beamlines will benefit from the support of the structural biology and high-pressure laboratories.

References

1. E. Karantzoulis, A. Carniel, S. Krecic, in *IPAC2014: Proceedings of the 5th International Particle Accelerator Conference, Dresden, Germany*, edited by Christine Petit-Jean-Genaz, Gianluigi Arduini, Peter Michel, Volker R.W. Schaa (JACoW, Geneva, Switzerland, 2014) p. 261.
2. M. Svandrlik *et al.*, in *IPAC2014: Proceedings of the 5th International Particle Accelerator Conference, Dresden, Germany*, edited by Christine Petit-Jean-Genaz, Gianluigi Arduini, Peter Michel, Volker R.W. Schaa (JACoW, Geneva, Switzerland, 2014) p. 2285.
3. E. Allaria *et al.*, Nat. Commun. **4**, 2476 (2013) doi: 10.1038/ncomms3476.
4. `http://www.elettra.eu/elettra-beamlines/xrd1.html`.
5. `http://www.elettra.eu/elettra-beamlines/mcx.html`.
6. `http://www.elettra.eu/elettra-beamlines/xrd2.html`.
7. `http://www.elettra.eu/elettra-beamlines/xpress.html`.
8. S. Bernstorff, E. Busetto, C. Gramaccioni, A. Lausi, L. Olivi, F. Zanini, A. Savoia, M. Colapietro, G. Portalone, M. Camalli, A. Pifferi, R. Spagna, L. Barba, A. Cassetta, Rev. Sci. Instrum. **66**, 1661 (1995) doi: 10.1063/1.1145875.
9. F. Cipriani *et al.*, Acta Cryst. D **62**, 1251 (2006) doi:10.1107/S0907444906030587.
10. L. Rebuffi, J.R. Plaisier, M. Abdellatief, A. Lausi, P. Scardi, Z. Anorg. Allg. Chem. **640**, 3100 (2014) doi: 10.1002/zaac.201400163.
11. P. Riello, A. Lausi, J. MacLeod, J.R. Plaisier, G. Zerauschek, P. Fornasiero, J. Synchrotron Radiat. **20**, 194 (2013) doi: 10.1107/S0909049512039246.
12. N. Poccia, M. Fratini, A. Ricci, G. Campi, L. Barba, A. Vittorini-Orgeas, G. Bianconi, G. Aeppli, A. Bianconi, Nat. Mater. **10**, 733 (2011) doi: 10.1038/nmat3088.
13. E. Nepovimova, E. Uliassi, J. Korabecny, L.E. Peña-Altamira, S. Samez, A. Pesaresi, G.E. Garcia, M. Bartolini, V. Andrisano, C. Bergamini, R. Fato, D. Lamba, M. Roberti, K. Kuca, B. Monti, M.L. Bolognesi, J. Med. Chem. **57**, 8576 (2014) doi: 10.1021/jm5010804.
14. V. Zannier, V. Grillo, F. Martelli, J.R. Plaisier, A. Lausi, S. Rubini, Nanoscale **6**, 8392 (2014) doi: 10.1039/C4NR01183J.